

## Anomalous Metallic State of $\text{Cu}_{0.07}\text{TiSe}_2$ : An Optical Spectroscopy Study

G. Li,<sup>1</sup> W. Z. Hu,<sup>1</sup> J. Dong,<sup>1</sup> D. Qian,<sup>2</sup> D. Hsieh,<sup>2</sup> M. Z. Hasan,<sup>2</sup> E. Morosan,<sup>3</sup> R. J. Cava,<sup>3</sup> and N. L. Wang<sup>1,\*</sup>

<sup>1</sup>*Beijing National Laboratory for Condensed Matter Physics, Institute of Physics, Chinese Academy of Sciences, Beijing 100080, People's Republic of China*

<sup>2</sup>*Department of Physics, Joseph Henry Laboratories of Physics, Princeton University, Princeton, New Jersey 08544, USA*

<sup>3</sup>*Department of Chemistry, Princeton University, Princeton, New Jersey 08544, USA*

(Received 8 January 2007; revised manuscript received 30 June 2007; published 17 October 2007)

We report an optical spectroscopy study on the newly discovered superconductor  $\text{Cu}_{0.07}\text{TiSe}_2$ . Consistent with the development from a semimetal or semiconductor with a very small indirect energy gap upon doping  $\text{TiSe}_2$ , it is found that the compound has a low carrier density. Most remarkably, the study reveals a substantial shift of the screened plasma edge in reflectance towards high energy with decreasing temperature. This phenomenon, rarely seen in metals, indicates either a sizable increase of the conducting carrier concentration or/and a decrease of the effective mass of carriers with reducing temperature. We attribute the shift primarily to the latter effect.

DOI: [10.1103/PhysRevLett.99.167002](https://doi.org/10.1103/PhysRevLett.99.167002)

PACS numbers: 74.25.Gz, 72.80.Ga, 78.20.-e

Charge density waves (CDW) and superconductivity are two important broken symmetry states in solids. The interplay between the two states has been a topic of central interest in condensed matter physics. Among various CDW materials, layered  $1T\text{-TiSe}_2$  is particularly interesting. The compound shows a lattice instability around 200 K, below which it enters into a commensurate CDW phase associated with a  $(2 \times 2 \times 2)$  superlattice [1–3]. Unlike the case of most CDW materials, the CDW transition in this compound is not driven by Fermi surface nesting. The ground state is believed to be either a semimetal or a semiconductor with a very small indirect gap [4–11]. It has recently been reported that, upon controlled intercalation of Cu into  $1T\text{-TiSe}_2$  to yield  $\text{Cu}_x\text{TiSe}_2$ , the CDW transition is continuously suppressed, and a superconducting state emerges near  $x = 0.04$ , with a maximum  $T_c$  of 4.15 at  $x = 0.08$  [12]. This is the first superconducting system realized in the  $1T$  structure CDW-bearing family. The CDW-superconductivity phase diagram developed for  $\text{Cu}_x\text{TiSe}_2$  is analogous to the antiferromagnetism-superconductivity phase diagram found for the high-temperature superconductors. The system offers a good opportunity to study the evolution of competing electronic states from CDW to superconductivity.

Recently, high quality single crystals have been successfully grown for the system. A detailed study of the superconducting properties has been performed on  $\text{Cu}_{0.07}\text{TiSe}_2$  single crystals [13]. It is of interest to investigate the electronic properties of the doped metallic phase. In this Letter, we report the first optical study on the superconducting compound  $\text{Cu}_{0.07}\text{TiSe}_2$ . Consistent with the development from a semimetal or semiconductor with a very small indirect energy gap upon doping, the study reveals that the compound has a low carrier density. Most remarkably, a substantial shift of the plasma edge in reflectance towards high energy with decreasing temperature is observed. This phenomenon, rarely seen in metals, indicates

either a sizable increase of the conducting carrier concentration or/and a decrease of the effective mass of carriers with reducing  $T$ . We conclude that the shift is mainly due to the latter effect.

Superconducting single crystals of  $\text{Cu}_{0.07}\text{TiSe}_2$  ( $T_c \sim 4$  K) with optically flat surfaces were grown via chlorine vapor transport, as described previously [13]. The frequency-dependent reflectance spectra  $R(\omega)$  at different  $T$  were measured by a Bruker IFS 66 v/s spectrometer in the range from 50 to 25 000  $\text{cm}^{-1}$  and a grating-type spectrometer from 20 000 to 50 000  $\text{cm}^{-1}$ . The sample was mounted on an optically black cone on the cold finger of a He flow cryostat. An *in situ* gold (50–15 000  $\text{cm}^{-1}$ ) and aluminum (9000–50 000  $\text{cm}^{-1}$ ) overcoating technique was employed for reflectance measurements. The Kramers-Kronig transformation of  $R(\omega)$  was used to obtain the other optical response functions. A Hagen-Rubens relation was used for low frequency extrapolation, and a constant extrapolation for high-frequency to 300 000  $\text{cm}^{-1}$  followed by a function of  $\omega^{-2}$  was used for the higher energy side.

Figure 1 shows the reflectance spectra at different temperatures: (a)  $R(\omega)$  spectra over very broad energy scale from 50 to 50 000  $\text{cm}^{-1}$  on a logarithmic scale; (b) the spectra in an expanded plot over the frequency range from 50 to 5000  $\text{cm}^{-1}$ . The  $R(\omega)$  values at low  $\omega$  are rather high and increase further with decreasing  $T$ . This is a typical metallic response. With increasing  $\omega$ ,  $R(\omega)$  drops quickly to a minimum value near 3000  $\text{cm}^{-1}$ , usually referred to as the “screened” plasma edge [11,14]. The relatively low edge position reveals a low carrier density. Most surprisingly, the plasma edge was found to display a substantial shift towards higher frequencies (i.e., a blueshift) with decreasing  $T$ . Above the edge frequency, the reflectance becomes roughly  $T$  independent. Near 15 000  $\text{cm}^{-1}$ , there is another edge structure in  $R(\omega)$ , which does not originate from the free-carrier plasmon, but is caused by an inter-

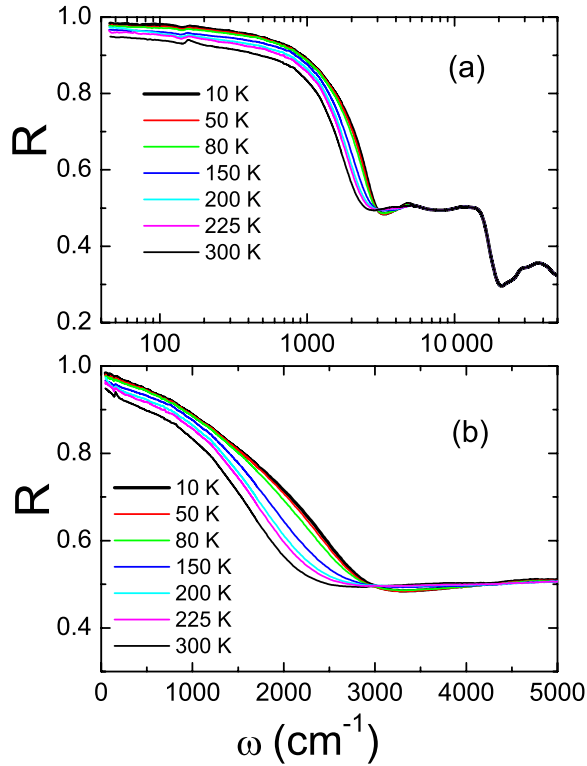


FIG. 1 (color online). (a) The  $T$ -dependent  $R(\omega)$  in the frequency range from 50 to 50 000  $\text{cm}^{-1}$  on a logarithmic scale. (b) The expanded plot of  $R(\omega)$  from 50 to 50 000  $\text{cm}^{-1}$ .

band transition. Besides these features, a phonon structure near  $140 \text{ cm}^{-1}$  can be clearly observed at high  $T$ . The feature weakens at low  $T$  due to increased screening by free carriers.

The formation of the plasma edge and its evolution with  $T$  is also reflected in the energy loss function,  $\text{Im}[-1/\epsilon(\omega)]$ , as shown in Fig. 2. In the energy loss function, the screened plasma frequency ( $\omega_p' = \omega_p/\sqrt{\epsilon_\infty}$ ) corresponds to the peak position, while the carrier damping (or scattering rate) is linked to the peak

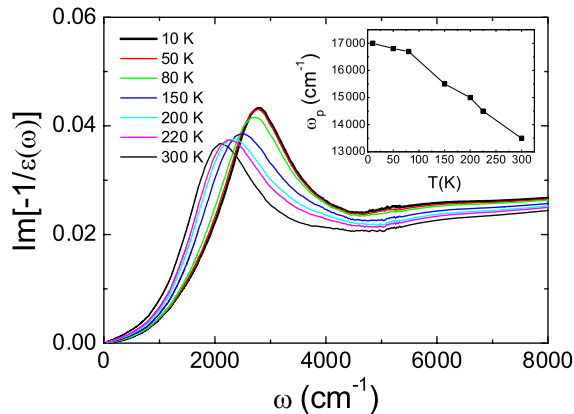


FIG. 2 (color online). The energy loss function spectra at different  $T$ . Inset: the unscreened plasma frequency obtained from the fit by Eq. (1) to reflectance data.

width. We can see clearly that, as  $T$  decreases from 300 to 10 K, the major change is the blueshift of the screened plasma frequency.

To analyze the variation of the carrier density and its damping quantitatively, we fit the experimental reflectance to a simple Drude-Lorentz model [15]:

$$\epsilon(\omega) = \epsilon_\infty - \frac{\omega_p^2}{\omega^2 + i\omega/\tau} + \sum_{i=1}^2 \frac{S_i^2}{\omega_i^2 - \omega^2 - i\omega/\tau_i}. \quad (1)$$

The model includes a Drude term and two Lorentz terms, which approximately capture the contributions by free carriers and interband transitions. A comparison of the measured  $R(\omega)$  and calculated curves at 300 and 10 K is shown in Fig. 3. In the inset, the experimental and calculated  $R(\omega)$  spectra at 300 K are displayed over broad frequency range. We find that this simple model can reasonably reproduce the  $R(\omega)$  curves. This is the case particularly for the spectrum at 300 K. At 10 K, the calculated curve deviates from the experimental spectrum at low  $\omega$ . This is understandable, considering that a constant parameter for scattering rate,  $1/\tau$  in the Drude term, is used for fitting. In reality, the carrier scattering rate (damping) may be  $\omega$ -dependent. The unscreened plasma frequencies,  $\omega_p$  of the Drude term, obtained at different  $T$  are shown in the inset of Fig. 2. The plasma frequency increases steadily from 13 500 to 17 000  $\text{cm}^{-1}$  with decreasing  $T$ , roughly a 20% increase. The scattering rate keeps roughly constant with  $1/\tau \sim 800\text{--}850 \text{ cm}^{-1}$ . In the analysis, the two Lorentz terms modeling the interband transitions are centered at 6500 and 14 500  $\text{cm}^{-1}$ , respectively. The epsilon infinity obtained is  $\epsilon_\infty = 18$ . Note that the value of the unscreened plasma frequency is fairly large, this is mainly due to the very small value of the effective mass. An estimation of the effective mass will be given below.

Figure 4 shows the optical conductivity  $\sigma_1(\omega)$  below 1000  $\text{cm}^{-1}$  at different  $T$ . A Drude-like conductivity is

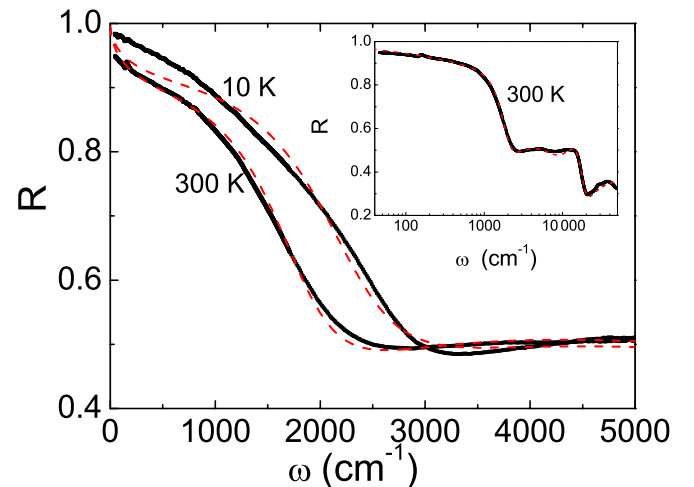


FIG. 3 (color online). The optical reflectance at 300 and 10 K, together with the fit by Eq. (1). Inset shows the spectra over a broad frequency range.

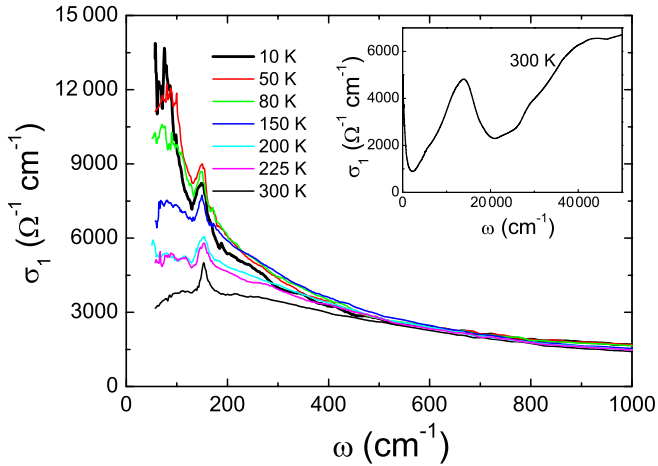


FIG. 4 (color online). Frequency dependence of the optical conductivity at different  $T$ . The inset shows the  $\sigma_1(\omega)$  at 300 K over a broad energy range.

present at low  $\omega$ , and its spectral weight [i.e., the area under the  $\sigma_1(\omega)$  curve] increases with decreasing temperature. This is expected, as the spectral weight of Drude-like conductivity is linked to effective conducting carrier density, consistent with the  $T$ -dependent evolution of both the reflectance and energy loss function spectra presented above. The inset shows the room- $T$   $\sigma_1(\omega)$  over a broad energy range. Besides the Drude component at low frequency, there exist several interband transition structures. The interband transition near  $6500 \text{ cm}^{-1}$  appears as a weak shoulder of the prominent peak near  $14500 \text{ cm}^{-1}$ . Stronger structures also appear at frequencies above  $20000 \text{ cm}^{-1}$ . All these features can be attributed to interband transitions from occupied Se  $4p$  bands to unoccupied parts of Ti  $3d$  bands in different momentum directions in  $\mathbf{K}$  space [16,17].

From the data presented above, we can see that the most striking property of this doped CDW material is the blueshift of the plasma frequency with decreasing  $T$ . Such a phenomenon is rarely seen in metals. Europium hexaboride ( $\text{EuB}_6$ ) is another prominent example showing a similar blueshift of the plasma edge [14]. However,  $\text{EuB}_6$  enters into a ferromagnetically ordered state below  $T_c \sim 16 \text{ K}$ : the blueshift of the plasma edge occurs only when the compound is cooled through the ferromagnetic transition. Moreover, the plasma frequency in  $\text{EuB}_6$  shifts to higher energy when a magnetic field is applied. Thus it is believed that the effect is related to the reduced scattering by spin ordering, or undressing effect as explained by Hirsch [18].  $\text{Cu}_{0.07}\text{TiSe}_2$  is, however, a superconductor and does not have any magnetic ordering.

It is well known that the plasma frequency is determined by the charge carrier density and the effective mass. In the case of a single band,  $\omega_p^2 = 4\pi n e^2 / m^*$ , the observed blueshift indicates either a sizable increase of carrier density or/and a reduction of the effective mass of the conducting charge carriers. However, it is unlikely that the carrier density changes with  $T$ , since the carrier density is a

quantity controlled by the valence electrons of the constituent atoms, and by the bond lengths of the lattice structure. One exception is a metal with a very low Fermi temperature ( $T_F$ ) due to a very small valence or/and conduction band crossing at  $E_F$ ; in that case the carrier number could be changed by thermal activation [19]. However, the number of such thermally activated carriers can only decrease with decreasing  $T$ , opposite to the trend observed here. Very recently, Hall effect measurements have been reported for Cu-doped  $\text{TiSe}_2$  crystals [20]. Indeed, it was found that the Hall coefficient  $R_H$  changes with  $T$  only for lightly Cu-doped samples, where CDW transitions exist. For the heavily Cu-doped samples, such as superconducting  $\text{Cu}_{0.07}\text{TiSe}_2$ ,  $R_H$  is  $T$  independent, which therefore rules out the possibility of a  $T$ -dependent carrier density.

As the carrier density does not change with  $T$ , we are left with the possibility that the effective mass of charge carriers decreases with decreasing  $T$ . From our observed plasma frequencies and the Hall coefficient results [20], we estimate that a mass reduction, from  $m^* = 0.55m_e$  to  $0.35m_e$ , occurs in  $\text{Cu}_{0.07}\text{TiSe}_2$  on cooling from 300 to 10 K. This behavior is in sharp contrast to many so-called strongly correlated electron systems that show an enhanced carrier effective mass at low  $T$  due to a many-body renormalization effect [15,21]. In order to get insight into this issue, it is necessary to examine the evolution of the band structure with Cu intercalation. The parent compound  $1T\text{-TiSe}_2$  is a well known CDW material. Its ground state is revealed to be either a low carrier density semimetal or a semiconductor with a very small indirect gap [4–11,16]. With the intercalation of  $\text{Cu}^{1+}$  into the structure, extra electrons are doped into the system. Within a rigid band picture, this will raise the chemical potential. Indeed, recent angle-resolved photoemission spectroscopy (ARPES) experiments indicate that Cu intercalation places the bottom of the Ti- $3d$  electron band near the  $L$  point further below  $E_F$  [22,23]. This electron band dominates the electronic properties, in agreement with the negative Hall and Seebeck coefficients seen in transport experiments [12,20].

It is noted that the electrons near  $L$  points couple strongly with lattice [24]. Then, a  $T$ -dependent electron-phonon coupling may cause a change of carrier effective mass. As the phonon number decreases with decreasing  $T$ , a reduced scattering of electrons from phonons (i.e., a mass reduction) is expected. In early studies on nontransition metals, such as Zn, a temperature shift of the mass renormalization arising from the electron-phonon interaction was observed [25] and well explained theoretically by Allen and Cohen [26]. However, this ordinary electron-phonon interaction has only a very small effect on the mass shift. It cannot explain the substantial change observed here. In fact, the  $L$  phonons are linked to the structural instability in the parent and slightly Cu-intercalated compounds. If strong phonon softening takes place at low  $T$ , one would expect to see an enhanced incoherent low-energy quasiparticle, opposite to the ordinary effect. Indeed, even for the present  $x = 0.07$  compound without

a static CDW instability, recent ARPES experiments indicate that the low- $T$  energy distribution curve (EDC) quasiparticle peak of the  $L$  pocket at a fixed  $k$  point near  $E_F$  does not become sharper after removing thermal effects [27]. Thus, a naive picture for a reduced electron-phonon interaction is not applicable here.

We propose following mechanism, which involves a  $T$ -induced band effect, for the mass change in this compound. We note that, for a system with a constant carrier density, the chemical potential is not fixed but shifts up with decreasing  $T$  when the Fermi energy of the system is not high. Assuming a degenerate electron gas for the metallic phase, the chemical potential has the following relation with  $T$ ,  $\mu \approx \mu_0[1 - \pi^2/12(T/T_F)^2]$ . For a usual metal, the Fermi temperature  $T_F$  is very high, and the  $T$ -induced change in  $\mu$  in the range 0–300 K is negligible. However, for the present case, the Fermi energy is rather low, about 80–100 meV at 300 K [27]. Then we expect to have an upward shift of chemical potential by about 5%–10% for  $T$  decreasing from 300 to 0 K. If the effective mass of electrons is different along the dispersive band, a change of effective mass at  $E_F$  could be caused by a chemical potential shift. As the  $L$  point is linked to the lattice instability, the electrons at the  $L$  point experience the strongest scattering. Away from the  $L$  point, along the dispersive band, the scattering would be significantly reduced. Indeed, from the ARPES experiment the EDC width at the  $L$  point (the band minimum) is much broader than other points away from the  $L$  point along the dispersive band [22,23]. Thus, an upward shift of chemical potential with decreasing  $T$ , driving the Fermi crossing point further away from the  $L$  point, would lead to a relatively smaller effective mass at  $E_F$ .

To summarize, we performed optical spectroscopy study on a newly discovered superconductor  $\text{Cu}_{0.07}\text{TiSe}_2$ . The study reveals it to be a low-carrier density metal, consistent with the development from a semimetal or semiconductor with a small indirect gap upon doping. Surprisingly, the data reveal a substantial shift of the plasma edge in reflectance towards high energy with decreasing  $T$ , a phenomenon rarely seen in metals. We attribute the observed  $T$ -dependent shift to an effective mass change related to the specific electron-phonon coupling near the  $L$  point and the small Fermi energy of the system.

We acknowledge very helpful discussions with Z. Q. Wang, L. Yin, D. L. Feng, Q. H. Wang, and Lu Yu. This work is supported by National Science Foundation of China, the Knowledge Innovation Project of Chinese Academy of Sciences, and the Ministry of Science and Technology of China. M. Z. H. and R. J. C. acknowledge partial support through NSF (No. DMR-0213706) and U.S. DOE No. DE-FG-02-05ER46200.

---

\*Corresponding author.  
nlwang@aphy.iphy.ac.cn

- [1] J. A. Wilson and A. D. Yoffe, *Adv. Phys.* **18**, 193 (1969).
- [2] J. A. Wilson, F. J. Di Salvo, and S. Mahajan, *Adv. Phys.* **24**, 117 (1975).
- [3] F. J. Di Salvo, D. E. Moncton, and J. V. Waszczak, *Phys. Rev. B* **14**, 4321 (1976).
- [4] R. Z. Bachrach, M. Skibowski, and F. C. Brown, *Phys. Rev. Lett.* **37**, 40 (1976).
- [5] M. M. Traum, G. Margaritondo, N. V. Smith, J. E. Rowe, and F. J. Di Salvo, *Phys. Rev. B* **17**, 1836 (1978).
- [6] O. Anderson, R. Manzyke, and M. Skibowski, *Phys. Rev. Lett.* **55**, 2188 (1985).
- [7] Th. Pillo, J. Hayoz, H. Berger, F. Levy, L. Schlapbach, and P. Aebi, *Phys. Rev. B* **61**, 16213 (2000).
- [8] T. E. Kidd, T. Miller, M. Y. Chou, and T.-C. Chiang, *Phys. Rev. Lett.* **88**, 226402 (2002).
- [9] K. Rossnagel, L. Kipp, and M. Skibowski, *Phys. Rev. B* **65**, 235101 (2002).
- [10] X. Y. Cui, H. Negishi, S. G. Titova, K. Shimada, A. Ohnishi, M. Higashiguchi, Y. Miura, S. Hino, A. M. Jahir, A. Titov, H. Bidadi, S. Nigishi, H. Namatame, M. Taniguchi, and M. Sasaki, *Phys. Rev. B* **73**, 085111 (2006).
- [11] G. Li, W. Z. Hu, D. Qian, D. Hsieh, M. Z. Hasan, E. Morosan, R. J. Cava, and N. L. Wang, *Phys. Rev. Lett.* **99**, 027404 (2007).
- [12] E. Morosan, H. W. Zandbergen, B. S. Dennis, J. W. G. Bos, Y. Onose, T. Klimczuk, A. P. Ramirez, N. P. Ong, and R. J. Cava, *Nature Phys.* **2**, 544 (2006).
- [13] E. Morosan, Lu Li, N. P. Ong, and R. J. Cava, *Phys. Rev. B* **75**, 104505 (2007).
- [14] L. Degiorgi, E. Felder, H. R. Ott, J. L. Sarrao, and Z. Fisk, *Phys. Rev. Lett.* **79**, 5134 (1997); S. Broderick, B. Ruzicka, L. Degiorgi, H. R. Ott, J. L. Sarrao, and Z. Fisk, *Phys. Rev. B* **65**, 121102 (2002); G. Caimi, A. Perucchi, L. Degiorgi, H. R. Ott, V. M. Pereira, A. H. Castro Neto, A. D. Bianchi, and Z. Fisk, *Phys. Rev. Lett.* **96**, 016403 (2006).
- [15] L. Degiorgi, *Rev. Mod. Phys.* **71**, 687 (1999).
- [16] A. Zunger and A. J. Freeman, *Phys. Rev. B* **17**, 1839 (1978).
- [17] A. H. Reshak and S. Auluck, *Phys. Rev. B* **68**, 245113 (2003).
- [18] J. E. Hirsch, *Phys. Rev. B* **62**, 14131 (2000).
- [19] B. I. Halperin and T. M. Rice, *Rev. Mod. Phys.* **40**, 755 (1968).
- [20] G. Wu, H. X. Yang, L. Zhao, X. G. Luo, T. Wu, G. Y. Wang, and X. H. Chen, *Phys. Rev. B* **76**, 024513 (2007).
- [21] N. L. Wang, J. J. McGuire, T. Timusk, R. Jin, J. He, and D. Mandrus, *Phys. Rev. B* **66**, 014534 (2002).
- [22] D. Qian, D. Hsieh, L. Wray, E. Morosan, N. L. Wang, Y. Xia, R. J. Cava, and M. Z. Hasan, *Phys. Rev. Lett.* **98**, 117007 (2007).
- [23] J. F. Zhao, H. W. Ou, G. Wu, B. P. Xie, Y. Zhang, D. W. Shen, J. Wei, L. X. Yang, J. K. Dong, X. H. Chen, and D. L. Feng, *Phys. Rev. Lett.* **99**, 146401 (2007).
- [24] M. Holt *et al.*, *Phys. Rev. Lett.* **86**, 3799 (2001).
- [25] Jesse J. Sabo, Jr, *Phys. Rev. B* **1**, 1325 (1970); S. Auluck, *ibid.* **9**, 5334 (1974).
- [26] P. B. Allen and M. L. Cohen, *Phys. Rev. B* **1**, 1329 (1970).
- [27] D. Qian *et al.* (unpublished).